Recursive phase estimation for image sharpening

M.P. Hayes and S.A. Fortune

Electrical and Computer Engineering Department, University of Canterbury,
Private Bag 4800, Christchurch, New Zealand.
Email: m.hayes@elec.canterbury.ac.nz

Abstract

Sharpness maximisation is a method that can be used to correct phase errors in images. In this paper we present a new recursive method to estimate the phase correction required for maximum image sharpness using the square of image pixel intensity metric S_2. This method avoids the optimisation step required by other image sharpening approaches. We also present a similar algorithm based on the solution to the sharpness gradient that is applicable to other sharpness measures. The new algorithm is significantly faster than other methods although the rate of convergence is still scene dependent.

Keywords: image contrast optimisation, image sharpening, autofocus, phase estimation

1 Introduction

Many imaging systems are affected by phase errors, resulting in image blurring. One example is astronomical images suffering degradation due to phase errors introduced by atmospheric turbulence [1]. It is also a major problem in coherent imagery; for example medical ultrasound images are degraded by tissue layers with inhomogeneous acoustic velocities [2], large array radar images are affected by structural flex over time [3], and synthetic aperture radar (SAR) and synthetic aperture sonar (SAS) images are degraded by platform motion [4, 5].

One method for estimating these phase errors is sharpness maximisation. Essentially the method perturbs a set of focus parameters so as to maximise an image quality metric of the calculated image. Different sharpness maximisation schemes can alter the set of focus parameters and how they relate to the image, the way image quality is measured, and the method by which the parameters are optimised.

Sharpness maximisation was first used by Muller and Buffington [1] to correct phase distortion in astronomical images. They showed that the simple sharpness metric

$$S_2 = \sum_{x,y} I[x,y]^2, \tag{1}$$

where $I[x,y]$ is the image intensity at pixel (x,y), is maximum for a correctly focused image. The aperture was divided into segments and a phase correction applied to each segment. The change in image sharpness was calculated and used to drive a derivative feedback correction scheme.

Paxman and Marron [6] showed the technique of sharpness maximisation could theoretically be applied to speckled coherent images such as synthetic aperture radar (SAR). Sharpness maximisation was then developed for spotlight SAR first by estimating a single motion parameter (acceleration) for a small image [7]. It was also applied to Inverse Synthetic Aperture Radar (ISAR) [8] and extended to higher order motions [9] and different sharpness measures [10].

The disadvantage of sharpness maximisation is that it is computationally intensive since it requires a multidimensional search over the set of focus parameters. In this paper we present a substantially faster recursive method. We start by stating the mathematical basis of sharpness maximisation in Section 2 and briefly review the standard approaches of sequential non-parametric sharpness maximisation, conjugate gradient sharpness maximisation, and parametric sharpness maximisation. In Section 3 we present our recursive method based on sequential non-parametric sharpness maximisation for the S_2 sharpness metric and then in Section 4 derive a more general algorithm by solving where the gradient of the image sharpness is zero. Some results showing the efficacy of the new method are shown in Section 5.

2 Sharpness maximisation

Consider a spotlight synthetic aperture system. Motion of the platform introduces a phase error resulting in range invariant blurring. The relationship between the blurred image $g[x,y]$ and the unblurred image $\bar{g}[x,y]$ is given by [4, 11]

$$g[x,y] = \bar{g}[x,y] \odot_y \mathcal{F}^{-1}_{v\to y}\left\{\exp\left(j\phi[v]\right)\right\}, \quad (2)$$

where $\phi[v]$ is the blurring phase function, $\odot_y$ denotes convolution in the y dimension, and $\mathcal{F}^{-1}_{v\to y}\{.\}$ denotes a discrete inverse Fourier transform. In the Fourier domain, the blurring can be succinctly described by

$$G[x,v] = \bar{G}[x,v]\exp\left(j\phi[v]\right), \quad (3)$$

where $\bar{G}[x,v]$ and $G[x,v]$ are discrete marginal Fourier transforms of $\bar{g}[x,y]$ and $g[x,y]$, i.e.,

$$G[x,v] = \frac{1}{N}\sum_y g[x,y]\exp\left(-j2\pi\frac{yv}{N}\right). \quad (4)$$

The key thing to note from Eq. (3) is that the phase error $\phi[v]$ is common to all ranges x.

The approach used by image sharpness maximisation to estimate $\phi[v]$ (and thus recover $\bar{g}[x,y]$ from $g[x,y]$) is to maximise some sharpness metric $\tilde{S}(\phi[v])$, i.e.,

$$\hat{\phi}[v] = \arg\max_{\phi[v]} \tilde{S}(\phi[v]). \quad (5)$$

Here $\tilde{S}(\phi[v])$ denotes the sharpness of the image $\tilde{g}[x,y,\phi[v]]$ obtained by applying a phase correction $\phi[v]$ to the blurred image, i.e.,

$$\tilde{g}[x,y,\phi[v]] = \mathcal{F}^{-1}_{v\to y}\left\{G[x,v]\exp\left(-j\phi[v]\right)\right\}. \quad (6)$$

Most sharpness metrics can be characterised by

$$S = \sum_{x,y} W[x]\Omega\left(I[x,y]\right), \quad (7)$$

where Ω describes a non-linear sharpness function applied to the image intensity $I = |g|^2$ at each point (for the effect of different metrics see [12]) and $W[x]$ is a range weighting function that weights the sharpness estimates for each x (for a choice of weighting function to increase the accuracy of the phase estimate see [13]), i.e.,

$$S = \sum_x W[x]S[x], \quad (8)$$

where

$$S[x] = \sum_y \Omega\left(|g[x,y]|^2\right). \quad (9)$$

Thus the phase $\hat{\phi}[v]$ that gives maximum image sharpness can be estimated using:

$$\hat{\phi}[v] = \arg\max_{\phi[v]} \sum_x W[x]\tilde{S}(x,\phi[v]), \quad (10)$$

where

$$\tilde{S}[x,\phi[v]] = N\sum_y \Omega\left(\left|\mathcal{F}^{-1}_{v\to y}\left\{G[x,v]\exp\left(-j\phi[v]\right)\right\}\right|^2\right). \quad (11)$$

There are many approaches to find the estimate $\phi[v]$ that maximises the image sharpness. In principle, the simplest method is to perform a multidimensional search for the N $\phi[v]$ values using Eq. (11) as the objective function. However, this is exceedingly slow.

2.1 Sequential non-parametric sharpness maximisation

Sequential non-parametric sharpness maximisation replaces a multidimensional search with a sequence of single dimensional searches. At each iteration, the phase of each spatial frequency is tweaked in turn to maximise the image sharpness. Denoting the spatial frequency of interest by v_0 and the applied phase correction by ϕ, the tweaked image sharpness is

$$\tilde{S}(x,v_0,\phi) = N\sum_y \Omega\left(\left|\mathcal{F}^{-1}_{v\to y}\left\{\tilde{G}[x,v,v_0,\phi]\right\}\right|^2\right), \quad (12)$$

where the tweaked image spectrum is

$$\tilde{G}[x,v,v_0,\phi] = \begin{cases} G[x,v]\exp\left(-j\phi\right) & v = v_0, \\ G[x,v] & \text{otherwise.} \end{cases} \quad (13)$$

An estimate of the phase correction, $\hat{\phi}$, at v_0 is then found by maximising a weighted sum of Eq. (12), i.e.,

$$\hat{\phi}[v_0] = \arg\max_{\phi} \sum_x W[x]\tilde{S}(x,v_0,\phi). \quad (14)$$

The image is then corrected with this phase estimate and the method repeated for each v_0 in v. A number of iterations are performed to ensure convergence due to the dependence of $\phi[\hat{v_0}]$ upon the choice of ϕ.

2.2 Conjugate gradient sharpness maximisation

For a spotlight synthetic aperture system, a closed-form expression can be obtained for the gradient (and Hessian) of the sharpness metric with respect to the phase-error parameters. This allows the use of a highly efficient conjugate-gradient search algorithm for the minimisation procedure [14, 11].

2.3 Parametric sharpness maximisation

While conjugate gradient methods speed up the search required for sequential non-parametric sharpness maximisation, it is faster to parameterise the set of focus parameters, say by using a Karhunen-Loeve decomposition [15, 16, 17]. This can substantially reduce the search space dimension or reduce the dependence between the focus parameters.

3 Recursive estimation of the phase of maximum sharpness

In this section we show how using the approach of non-parametric sharpness maximisation for the common S_2 sharpness measure, the phase estimate giving maximum image sharpness can be recursively estimated without having to use a search.

The S_2 sharpness measure sums the squares of the image intensities, i.e., $\Omega(I) = I^2$. Considering the sharpness for a single range x, then from Eq. (9)

$$S_2[x] = \sum_y |g[x,y]|^4 . \tag{15}$$

Using the Fourier autocorrelation and energy theorems the S_2 image sharpness can be calculated using

$$\begin{aligned} S_2[x] &= N \sum_{v_2} \left| \sum_{v_1} G[x,v_1] G^*[x,v_1 - v_2] \right|^2 , \\ &= N \sum_d \left| \sum_v G[x,v] G^*[x,v-d] \right|^2 , \\ &= N \sum_d |GG[x,d]|^2 , \end{aligned} \tag{16}$$

where $GG[x,d]$ is the marginal 1-D autocorrelation of $G[x,v]$ at lag d for range x, i.e.,

$$\begin{aligned} GG[x,d] &= \sum_v G[x,v] G^*[x,v-d] \\ &= \frac{1}{N} \sum_y |g[x,y]|^2 \exp\left(-j2\pi \frac{yv}{N}\right) . \end{aligned} \tag{17}$$

Using this result for the S_2 measure, Eq. (12) simplifies to

$$\tilde{S}_2[x,v_0,\phi] = N \sum_d \left| \tilde{GG}[x,d,v_0,\phi] \right|^2 . \tag{18}$$

After straightforward but tedious mathematics, the sharpness can be expressed as a function of the phase correction ϕ,

$$\begin{aligned} \tilde{S}_2[x,v_0,\phi] = \; & S_2[x] + 8E[x] \left|G[x,v_0]\right|^2 (1 - \cos\phi) \\ & + 4N \mathcal{R}\left\{K[x,v_0] \left(\exp(-j\phi) - 1\right)\right\} \\ & + 2N \mathcal{R}\left\{L[x,v_0] \left(\exp(-j\phi) - 1\right)^2\right\} \\ & - 2N \left|G[x,v_0]\right|^4 \left[3 + \mathcal{R}\left\{\exp(j2\phi) - 4\exp(j\phi)\right\}\right] , \end{aligned} \tag{19}$$

where $\mathcal{R}\{z\}$ denotes the real part of z, $E[x]$ is the image energy at each range (invariant under blurring),

$$\begin{aligned} E[x] &= \sum_y |g[x,y]|^2 = N \sum_v |G[x,v]|^2 \\ &= NGG[x,0], \end{aligned} \tag{20}$$

and where

$$\begin{aligned} K[x,v_0] &= G[x,v_0] \sum_d GG[x,d] G^*[x,v_0+d], \\ L[x,v_0] &= G^2[x,v_0] \sum_d G^*[x,v_0-d] G^*[x,v_0+d]. \end{aligned} \tag{21}$$

The phase of K is a high order, weighted, phase difference estimate at v_0 while the phase of L is is a high order, weighted, phase curvature estimate at v_0.

Expanding Eq. (19) yields

$$\begin{aligned} \tilde{S}_2[x,v_0,\phi] = \; & S_2[x] + 8E[x] \left|G[x,v_0]\right|^2 \\ & - 4N \mathcal{R}\left\{K[x,v_0]\right\} + 2N \mathcal{R}\left\{L[x,v_0]\right\} \\ & - 6N \left|G[x,v_0]\right|^4 + 4N \mathcal{R}\left\{K[x,v_0] \exp(-j\phi)\right\} \\ & - 4N \mathcal{R}\left\{L[x,v_0] \exp(-j\phi)\right\} \\ & + 2N \mathcal{R}\left\{L[x,v_0] \exp(-j2\phi)\right\} \\ & - 2N \left|G[x,v_0]\right|^4 \cos(2\phi) \\ & + 8N \left|G[x,v_0]\right|^4 \cos(\phi) \\ & - 8E[x] \left|G[x,v_0]\right|^2 \cos(\phi), \end{aligned} \tag{22}$$

and considering only the dominant terms that vary with ϕ,

$$\tilde{S}_2'[x,v_0,\phi] \approx 4N \mathcal{R}\left\{\chi[x,v_0] \exp(-j\phi)\right\} , \tag{23}$$

where

$$\chi[x,v_0] = K[x,v_0] + L[x,v_0] - 2E[x] \left|G[x,v_0]\right|^2 . \tag{24}$$

The phase estimate $\hat{\phi}$ that maximises the image sharpness is equivalent to maximising a weighted sum of the real part of χ, i.e.,

$$\hat{\phi}[v_0] = \arg\max_\phi \sum_x W[x] \mathcal{R}\left\{\chi[x,v_0] \exp(-j\phi)\right\} , \tag{25}$$

or equivalently when the weighting $W[x]$ is real

$$\hat{\phi}[v_0] = \arg\max_\phi \mathcal{R}\left\{\sum_x W[x] \chi[x,v_0] \exp(-j\phi)\right\} . \tag{26}$$

Thus the phase estimate $\hat{\phi}$ can be directly calculated using

$$\hat{\phi}[v_0] = \mathcal{P}\left\{\sum_x W[x] \chi[x,v_0]\right\} , \tag{27}$$

where $\mathcal{P}\{z\}$ denotes the phase (or argument) of z.

When the image spectrum is highly correlated and $N \gg 1$, then to a good approximation

$$\chi[x,v_0] \approx K[x,v_0], \tag{28}$$

and thus a direct estimate of ϕ can be obtained using

$$\hat{\phi}[v_0] \approx \mathcal{P}\left\{\sum_x W[x]G[x,v_0]H^*[x,v_0]\right\}, \quad (29)$$

where

$$H[x,v] = \mathcal{F}_{y\to v}\left\{|g[x,y]|^2\, g[x,y]\right\}. \quad (30)$$

Here $\mathcal{F}_{y\to v}\{.\}$ denotes a discrete Fourier transform evaluated at a spatial frequency sample v.

A significant speed advantage can be obtained by computing all N phase estimates $\hat{\phi}[v]$ in parallel using

$$\hat{\phi}[v] \approx \mathcal{P}\left\{W[x]G[x,v]H^*[x,v]\right\}. \quad (31)$$

This greatly reduces the number of Fourier transforms. However, since the effects of the phases on the image sharpness are not independent, iteration is required to find the phase that gives maximum image sharpness.

4 Image sharpness gradient

Let's now consider a phase correction $\phi[v]$ applied to all spatial frequencies v at once, so

$$\tilde{G}[x,v] = G[x,v]\exp\left(-j\phi[v]\right). \quad (32)$$

The sharpness of the corrected image is

$$\tilde{S} = \sum_{x,y} W[x]\Omega\left(|\tilde{g}[x,y]|^2\right), \quad (33)$$

with a gradient, given by [5],

$$\begin{aligned}\frac{\partial \tilde{S}}{\partial \phi[v]} = \; & 2\sum_{x,y} W[x]\frac{\partial \Omega}{\partial \tilde{I}} \\ & \times \mathcal{I}\left\{\tilde{g}^*[x,y]\tilde{G}[x,v]\exp\left(j2\pi\frac{vy}{N}\right)\right\},\end{aligned} \quad (34)$$

where $\mathcal{I}\{z\}$ denotes the imaginary part of z. Provided the weighting $W[x]$ is real, then Eq. (34) can be written as

$$\frac{\partial \tilde{S}}{\partial \phi[v]} = 2\,\mathcal{I}\left\{\sum_x W[x]\tilde{G}[x,v]\tilde{H}^*_\Omega[x,v]\right\}, \quad (35)$$

where

$$\tilde{H}_\Omega[x,v] = \mathcal{F}_{y\to v}\left\{\frac{\partial \Omega}{\partial \tilde{I}}\tilde{g}[x,y]\right\}. \quad (36)$$

Substituting Eq. (32), the gradient Eq. (35) becomes

$$\frac{\partial \tilde{S}}{\partial \phi[v]} = 2\,\mathcal{I}\left\{\sum_x W[x]G[x,v]\tilde{H}^*_\Omega[x,v]\exp\left(-j\phi[v]\right)\right\}, \quad (37)$$

then after equating the gradient to zero, the phase correction $\hat{\phi}[v]$ giving minimum or maximum sharpness can be found. For $\Omega(I) = I^\beta$ where $\beta > 1$, the phase estimate giving maximum sharpness is

$$\hat{\phi}[v] = \mathcal{P}\left\{\sum_x W[x]G[x,v]\tilde{H}^*_\Omega[x,v]\right\}. \quad (38)$$

Note Eq. (38) has to be solved recursively since $\tilde{g}[x,y]$, and thus $\tilde{H}_\Omega[x,v]$, depends on the phase correction $\phi[v]$. For example, the S_2 sharpness measure $\Omega(\tilde{I}) = \tilde{I}^2$ has $\partial\Omega(\tilde{I})/\partial\tilde{I} = 2\tilde{I}$ and so

$$\tilde{H}_\Omega[x,v] = \mathcal{F}_{y\to v}\left\{|\tilde{g}[x,y]|^2\,\tilde{g}[x,y]\right\}. \quad (39)$$

It is worth noting the similarity of Eq. (39) with Eq. (30). Essentially the difference is due to whether the phases at all spatial frequencies are estimated and corrected in parallel or whether the phase at each spatial frequency is estimated and corrected sequentially.

Another common sharpness measure, good at sharpening shadows, is $\Omega(\tilde{I}) = -\tilde{I}^{1/2}$ [12]. Here $\partial\Omega(\tilde{I})/\partial\tilde{I} = -1/(2\tilde{I}^{1/2}) = -1/(2\,|\tilde{g}|)$ and thus

$$\tilde{H}_\Omega[x,v] = -\mathcal{F}_{y\to v}\left\{\frac{\tilde{g}[x,y]}{2\,|\tilde{g}[x,y]|}\right\}. \quad (40)$$

Finally, a promising sharpness measure is the negative of the image entropy [12], where $\Omega(\tilde{I}) = \tilde{I}\log\tilde{I}$, $\partial\Omega(\tilde{I})/\partial\tilde{I} = -\left(1+\log\tilde{I}\right)$, and so

$$\tilde{H}_\Omega[x,v] = -\mathcal{F}_{y\to v}\left\{\tilde{g}[x,y]\left(1+2\log|\tilde{g}[x,y]|\right)\right\}. \quad (41)$$

5 Results

The convergence of the sharpness using recursive phase estimation is shown in Fig. 1. Two test images were utilised: one consisting of several point targets and the other consisting of a rippled surface. The algorithm converges much faster for the point target image; this is consistent with other autofocus algorithms [13].

To evaluate the performance of the recursive method a distributed target consisting of a square block with coherent speckle noise was simulated and a known 1-D phase error was introduced. The phase was then estimated using the new recursive method and a number of standard methods. As shown in Fig. 2, all methods essentially estimated the same phase error (shown as phase differences to remove any inconsequential linear phase bias). The number of evaluations of the objective function is shown in Fig. 3 and the elapsed CPU time is shown in Table 1. This shows that the new algorithm is substantially faster than the other algorithms.

Method	Search space	Iterations	CPU time (s)
Direct (recursive)	256 direct estimates	20	30
Gradient non-parametric	256 dimensional search	1	1500
Sequential non-parametric	256 1D searches	20	18000

Table 1: CPU time required to converge to solution for different sharpness maximisation methods.

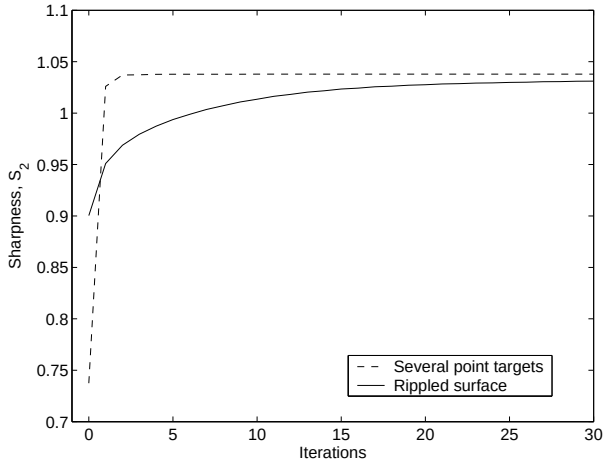

Figure 1: Convergence of sharpness using recursive phase estimation. Uses image consisting of several point targets and image consisting of rippled surface. Sharpness is normalised to unity for aberration free image.

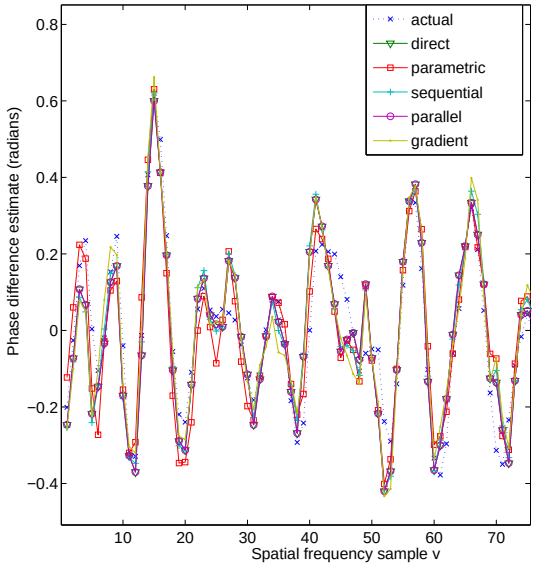

Figure 2: The phase estimated by sharpness maximisation techniques: recursive (direct), parametric multidimensional optimisation, sequential non-parametric optimisation (sequential), parallel non-parametric optimisation (parallel), and non-parametric conjugate gradient multidimensional optimisation (gradient).

6 Discussion

With a unity weighting $W[x] = 1$, Eq. (29) for the S_2 recursive sharpness maximisation can be expanded into

$$\hat{\phi}[v_0] = \mathcal{P}\left\{\sum_{x,d} GG[x,d]G[x,v_0]G^*[x,v_0+d]\right\}. \tag{42}$$

For a single separation d, this becomes

$$\hat{\phi}[v_0,d] = \mathcal{P}\left\{\sum_{x} GG[x,d]G[x,v_0]G^*[x,v_0+d]\right\}, \tag{43}$$

which is a weighted phase difference estimation, or shear average. Thus recursive maximisation of S_2 corrects the phase of a single echo by a combined weighted phase difference estimation over all separations. This could be considered a method of high-order echo-correlation. By measuring the phase difference between all other echos, then correcting by a weighted average of that difference, the mean difference between the phase of this echo and all others is minimised. The mean echo phase is *straightened*, increasing the sharpness of the image. The method of sharpness maximisation is compared to echo-correlation in [13].

7 Conclusions

In this paper we have presented a new algorithm for the autofocus of synthetic aperture spotlight imagery. It recursively estimates the phase error without having to perform an optimisation search and thus is significantly faster than traditional methods. The algorithm was derived using two different approaches for the S_2 sharpness measure and was found to show that sharpness maximisation with the S_2 sharpness measure is equivalent to high-order echo-correlation.

References

[1] R. A. Muller and A. Buffington, "Real-time correction of atmospherically degraded telescope images through image sharpening," *Journal of the Optical Society of America*, vol. 64, pp. 1200–1210, Sept. 1974.

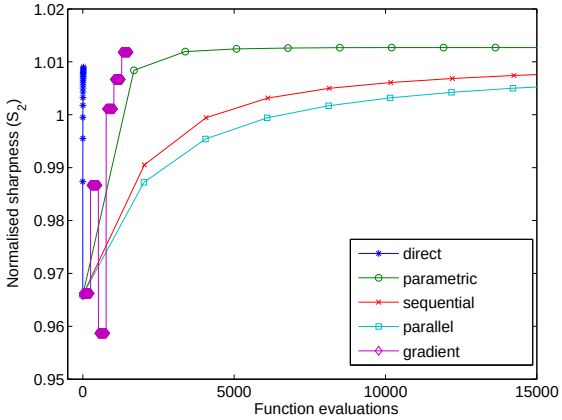

Figure 3: Comparison of the number of evaluations of the objective function for different sharpness maximisation methods. Note all methods have oversharpened the image indicated by the normalised sharpness being greater than 1.

[2] L. Nock, G. Trahey, and S. Smith, "Phase aberration correction in medical ultrasound using speckle brightness as a quality factor," *Journal of the Acoustics Society of America*, vol. 85, pp. 1819–1833, May 1989.

[3] E. H. Attia and B. D. Steinberg, "Self-cohering large antenna arrays using the spatial correlation properties of radar clutter," *IEEE Transactions on Antennas and Propagation*, vol. 37, pp. 30–38, Jan. 1989.

[4] J. C. Curlander and R. N. McDonough, *Synthetic Aperture Radar: Systems and signal processing*. New York: John Wiley and sons, 1996.

[5] P. T. Gough and D. W. Hawkins, "Imaging algorithms for a strip-map synthetic aperture sonar: Minimizing the effects of aperture errors and aperture undersampling," *IEEE Journal of Oceanic Engineering*, vol. 22, pp. 27–39, January 1997.

[6] R. G. Paxman and J. C. Marron, "Aberration correction of speckled imagery with an image-sharpness criterion," *Statistical Optics*, vol. 976, pp. 37–47, 1998.

[7] D. Blacknell, A. P. Blake, C. J. Oliver, and R. G. White, "A comparison of SAR multilook registration and contrast optimisation autofocus alogrithms applied to real SAR data," in *International Radar Conference*, pp. 363–366, 1992.

[8] F. Berizzi and G. Corsini, "Autofocusing of inverse synthetic aperture radar images using contrast optimization," *IEEE Transactions on Aerospace and Electronic Systems*, vol. 32, pp. 1185–1191, July 1996.

[9] F. Berizzi, G. Corsini, M. Diani, and M. Veltroni, "Autofocus of wide azimuth angle SAR images by contrast optimisation," in *International Geoscience and Remote Sensing Symposium*, vol. 2, pp. 1230–1232, 1996.

[10] L. Xi, L. Guosui, and J. Ni, "Autofocusing of ISAR images based on entropy minimization," *IEEE Transactions on Aerospace and Electronic Systems*, vol. 35, pp. 1240–1252, October 1999.

[11] J. Fienup, "Synthetic-aperture radar autofocus by maximizing sharpness," *Optics Letters*, vol. 25, pp. 221–223, February 2000.

[12] J. R. Fienup and J. J. Miller, "Aberration correction by maximizing generalized sharpness metrics," *Journal of the Optical Society of America A*, vol. 20, pp. 609–620, April 2003.

[13] S. A. Fortune, *Phase error estimation for synthetic aperture imagery*. PhD thesis, Department of Electrical and Computer Engineering, University of Canterbury, 2005.

[14] P. T. Gough and R. G. Lane, "Autofocussing SAR and SAS images using a conjugate gradient search algorithm," in *Proceedings of International Geoscience and Remote Sensing Symposium, 1998*, vol. 2, pp. 621–623, IEEE, 1998.

[15] S. A. Fortune, P. T. Gough, and M. P. Hayes, "A statistical method for autofocus of synthetic aperture sonar images," in *IVCNZ2000, Image and Vision Computing New Zealand*, (Hamilton, New Zealand), pp. 56–61, November 2000.

[16] S. A. Fortune, P. T. Gough, and M. P. Hayes, "Statistical autofocus of synthetic aperture sonar images using image contrast optimisation," in *IGARSS2001, International Geoscience and Remote Sensing Symposium*, (Sydney, Australia), July 2001.

[17] S. A. Fortune, P. T. Gough, and M. P. Hayes, "Statistical autofocus of bathymetric, multiple-frequency synthetic aperture sonar images using image contrast optimisation," in *Oceans 2001*, (Honolulu, Hawaii), pp. 163–169, November 2001.